ACS Medicinal Chemistry Letters
Cite This: ACS Med. Chem. Lett. 2019, 10, 1609−1613
Letter
pubs.acs.org/acsmedchemlett

In Silico Discovery of JMJD6 Inhibitors for Cancer Treatment

Ting Ran,[†,‡,⊥] Rongquan Xiao,[†,⊥] Qixuan Huang,[†] Haoliang Yuan,[¶] Tao Lu,[§] and Wen Liu*[,†]

[†]Fujian Provincial Key Laboratory of Innovative Drug Target Research, School of Pharmaceutical Sciences, Xiamen University, Xiamen, Fujian 361102, China

[‡]Department of Chemical Biology, College of Chemistry and Chemical Engineering, Xiamen University, Xiamen, Fujian 361105, China

[¶]Jiangsu Key Laboratory of Drug Discovery for Metabolic Disease and State Key Laboratory of Natural Medicines, China Pharmaceutical University, Nanjing, Jiangsu 210009, China

[§]State Key Laboratory of Natural Medicines, China Pharmaceutical University, Nanjing, Jiangsu 210009, China

Supporting Information

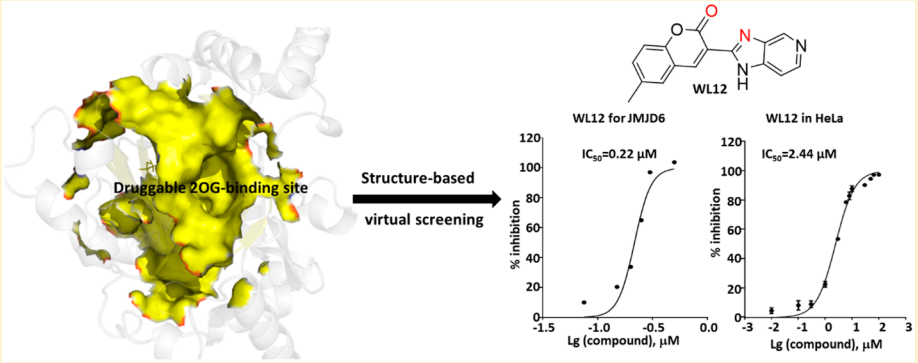

ABSTRACT: The 2-oxoglutarate (2OG)-dependent oxygenase JMJD6 is emerging as a potential anticancer target, but its inhibitors have not been reported so far. In this study, we reported an in silico protocol to discover JMJD6 inhibitors targeting the druggable 2OG-binding site. Following this protocol, one compound, which we named as WL12, was found to be able to inhibit JMJD6 enzymatic activity and JMJD6-dependent cell proliferation. To our best knowledge, this is the first case in drug discovery targeting JMJD6.

KEYWORDS: *JMJD6, inhibitors, in silico, cancer treatment*

Jumonji C (JmjC) domain-containing proteins belong to the 2-oxoglutarate (2OG)-dependent oxygenase superfamily. Most of them possess lysine demethylase (KDM) activity,[1] while some were acknowledged as protein hydroxylases.[2,3] Recently, several KDMs were also identified to be arginine demethylases (RDM).[4] The diverse enzymatic functions are all executed by the JmjC domain that forms a catalytic site for 2OG-Fe (II) binding. Nowadays, the JmjC domain-containing protein family has emerged as a new "star" in targeted-drug discovery due to their diverse functions in human diseases, particularly cancers. The enzymatic activity of JmjC domain-containing proteins was often shown to be essential for its function. Therefore, targeting the catalytic site was suggested to be an effective way to interfere with their carcinogenic function.[5] For example, KDM5 inhibitor, EPT-103182, has entered early preclinical study.[6]

JMJD6, the only arginine demethylase validated both *in vitro* and in cultured cells,[7] has been reported to be involved in cancer development, including melanoma,[8] colon cancer,[9] lung cancer,[10] liver cancer,[11] and breast cancer.[12] Moreover, the enzymatic activity of JMJD6 was found to be essential for its function in cancer development. JMJD6 acts as a transcriptional and splicing regulator through arginine demethylation or lysine hydroxylation on both histones and nonhistone proteins. Therefore, inhibiting the enzyme activity of JMJD6 is believed to be a feasible solution for treatment of cancers where JMJD6 is involved. However, such inhibitors are yet to be discovered, highlighting the urgency to develop new strategies for JMJD6-targeted drug discovery.

In this study, the druggability of JMJD6 was first computationally evaluated by elaborating the structure of the JmjC domain of JMJD6. We then developed an in silico protocol for virtual screening, aiming to rapidly discover small-molecule inhibitors targeting the active site of JMJD6. The hit compounds obtained by virtual screening were biologically validated in terms of their inhibition on the demethylation activity of JMJD6 and on the JMJD6-dependent cancer cell proliferation. To our best knowledge, this is the first time to

Received: June 12, 2019
Accepted: November 19, 2019
Published: November 19, 2019

DOI: 10.1021/acsmedchemlett.9b00264
ACS Med. Chem. Lett. 2019, 10, 1609−1613

exploit the therapeutic potential of JMJD6 as anticancer target through small-molecule inhibitor discovery.

Currently, most of the inhibitors targeting members in the JmjC domain-containing protein family exert their inhibitory activity by competing with 2OG binding, and they are defined as 2OG-competitive inhibitors. We therefore tested the druggability of the 2OG-binding site in JMJD6 by analyzing the crystal structures (PDB IDs: 3k2o,[14] 3ldb,[13] 3ld8,[13] 6fqc) of its JmjC domain. It is known that the JmjC domains share a conserved double-stranded β-helix (DSBH) fold,[15] which is composed of central β sheets (β6~β13) and peripheral α helixes (α1~α15) in JMJD6 protein (Figure 1A).[16] The

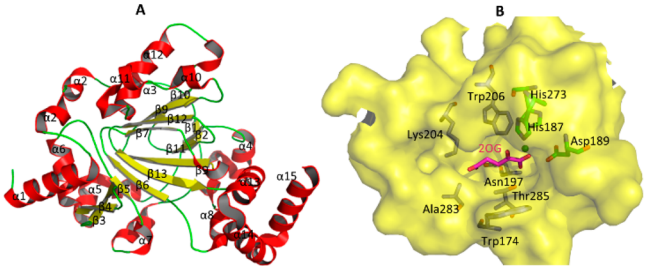

Figure 1. (A) Secondary structure of the JmjC domain in JMJD6 (3ldb).[13] α helixes, β sheets, and loops were depicted in red, yellow, and green, respectively. (B) Protein surface of the central β sheets (3ldb).[13] 2OG, the catalytic triad residues and other representative residues forming the 2OG-binding sites were depicted by magenta, yellow, and blue sticks, respectively.

central β sheets (amino acids 173 to 211 and 255 to 288 in JMJD6) are responsible for binding with 2OG through shaping a buried cavity (Figure 1B). The sequence of the JmjC domain is highly similar between JMJD6 and other JmjC domain-containing proteins (Figure S1). Histidine 187 (His187), aspartic acid 189 (Asp189), and histidine 273 (His273) on the β sheets form an iron-chelated catalytic triad to anchor 2OG, which is highly conserved (Figure S1).[17,18] Many other residues are also involved in forming the 2OG-binding site in JMJD6 (Figure 1B). Alignment of four independent crystal structures of the JmjC domain complexed with different ligands, such as 2-OG and NOG, gave small root-mean-square deviations (RMSDs), suggesting that the JmjC domain of JMJD6 is conformationally stable (Table S1). Stability of the JmjC domain was further suggested by MD simulations of apo- and holo-structures, which revealed a narrow RMSD window from 1.0 to 3.0 Å relative to the crystal structures (Figure S2A). RMSF of αC atoms demonstrated that the central β sheets were especially stable than other regions (Figure S2B).

We then performed druggability analysis of JMJD6 by using SiteMap[19] and FTMAP[20] methods. All crystal structures and representative frames extracted from the MD trajectories based on conformational clustering were used for the analysis. SiteMap analysis showed that the 2OG-binding site was the most likely druggable pocket due to its highest Dscore (Table S2). Other structural characteristics were also acceptable as a druggable pocket for the 2OG-binding site (Table S3). As shown in Figure S3A, white dots representing the space capable of grasping small-molecule ligands were distributed consecutively from the core 2OG-binding region to the outer regions near the L1 loop linking β3 and β4 and C-terminal helixes (α13–α15). Hydrophobic regions that were important for the binding of drug-like compounds were also distributed consecutively in a large part of the cavity. Taken together, the 2OG-binding site might be a potential druggable pocket. The pocket analysis by FTMAP, an alternative algorithm, was consistent with the SiteMap outcome (Figure S4). It was worth to note that SiteMap analysis revealed some other sites on the protein surface as potential allosteric sites.[21−23] However, these sites had smaller Dscores than the 2OG-binding site (Table S2) and significantly smaller volume than what is needed for a druggable pocket, exemplified by the site formed by α1, α2, and α6 helices that had the second highest Dscore (Figure S3B and Table S4). Similar results were also obtained from the AlloSite analysis (Figure S5).[24]

According to the analysis described above, the core 2OG-binding region is superior to other regions in terms of druggability, and virtual screening was carried out targeting this region. To ensure the accuracy of our virtual screening, we constructed a model based on protein−ligand interactions. As JMJD6 inhibitors have not been reported yet, we docked the scaffold moieties of the 2OG-competitive inhibitors targeting other JmjC domain-containing proteins to JMJD6 to generate protein−ligand interactions by the Glide docking method (Figure 2A and Figure S6).[25] The scaffolds were chosen for

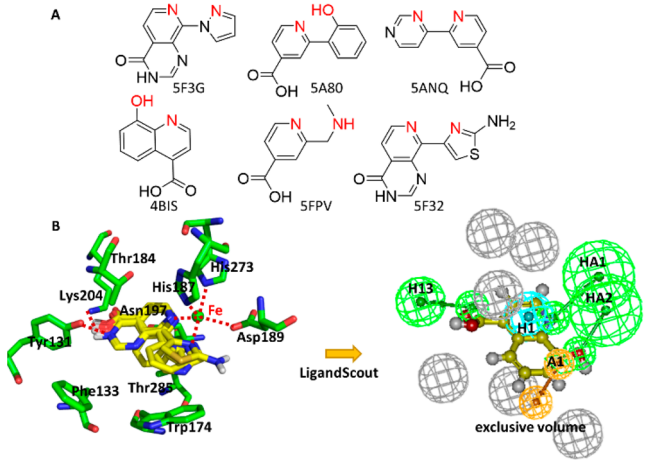

Figure 2. (A) Scaffold structures of known 2OG-competitive inhibitors targeting other JmjC domain-containing proteins. (B) Diagram for generating structure-based pharmacophore model. Hydrogen-bonds (HBs) were shown as firebrick lines, and residues were shown as green sticks (3ldb).[13] H1 was a hydrophobic feature, and A1 was an aromatic ring feature (right panel). HA1−HA3 were hydrogen-bond acceptor features. Gray spheres represent EVS that account for steric clashes of residues.

pharmacophore generation as they were located at the core 2OG-binding region when binding with other JmjC domain-containing proteins and were responsible for the coordination interaction with iron ion (Figure S7).[26−29] Thus, we hypothesized that they could play a similar role in the binding with JMJD6. As expected, all scaffolds were able to be chelated with iron with at least one coordination interaction (Figure 2B). Meanwhile, more than one HB with Tyr131, Asn197, or Lys204 was observed, which was shown to be important for ligand binding in FTMAP analysis as described above. Moreover, all scaffolds possessed aromatic rings located at the hydrophobic regions around the iron ion identified by the SiteMap analysis. These interaction features perfectly matched the structural properties of the core 2OG-binding region of JMJD6, indicating that ligands with similar interaction features

DOI: 10.1021/acsmedchemlett.9b00264
ACS Med. Chem. Lett. 2019, 10, 1609−1613

to these scaffolds probably have the capability to bind to JMJD6.

Next, the docking poses of the scaffolds were used for the generation of interaction pharmacophore model with LigandScout,[30] which was a commonly used tool to extract interaction features based on protein−ligand binding. The pharmacophore features extracted from each JMJD6-scaffold complex were clustered, which finally derived a pharmacophore model with two HB acceptor features corresponding to the coordination interaction with metal ion, one HB acceptor feature projected to Lys204, one hydrophobic feature located between the metal ion and Tyr131 or Phe133, and one aromatic feature corresponding to Trp174 (Figure 2B). Among these features, the coordination interaction with metal ion was set as an essential feature in our virtual screening below, which appeared in all 2OG-competitve inhibitors. These features combined with excluding volume spheres (EVS) basically covered the druggable regions as well as important interaction sites revealed by the SiteMap and FTMAP analysis. This pharmacophore model was subsequently applied to screen several diversity and fragment libraries with a total of about 0.9 million compounds (see Supporting Information for details). As a result, 7530 compounds passed the screening by the pharmacophore model with the FitValues ranging from 0 to 4. Among them, 5198 compounds were mapped to at least three features. Moreover, most of them possessed the HA1 or HA2 features that corresponded to the coordination interaction with metal ion. These compounds were further docked into the 2OG-binding site of JMJD6. On the basis of molecular docking, 577 compounds were selected for further evaluation, including the ones with better docking score than previously used scaffolds, similar poses between the Glide docking and pharmacophore mapping, or metal-chelated docking pose identified by visual inspection. Most selected compounds had acceptable drug-like properties (Figure S8). Considering structural classification, pharmacophore mapping, docking score, and drug-like properties, 12 non-PAINS[31] and purchasable compounds belonging to five types of scaffolds were finally chosen for biological evaluation, which we named WL1 to WL12 (Figure S9).

We then tested the activity of these compounds in inhibiting JMJD6 demethylase activity by enzymatic assays. As shown in Figure 3A, compounds WL1, WL2, WL8, WL9, WL10, WL11, and WL12 inhibited the demethylase activity of JMJD6 as examined by the demethylation assay followed by immunoblotting. Subsequently, we investigated the antiproliferation effects of these compounds in HeLa and SMCC7721 cells in which JMJD6 has been shown to play a vital role.[11,32,33] It was found that only WL12 exhibited antiproliferation effects. The IC_{50} values for WL12 in HeLa and SMCC7721 cells were 2.44 and 10.18 μM, respectively (Figure 4B,C). Importantly, this compound exhibited selectivity over normal cells, such as L02 hepatocyte cells (Figure S10). We then focused on investigating the activity of compound WL12 in biochemical assays and in cultured cells. First, the IC_{50} of WL12 targeting JMJD6 was measured by demethylation assay (formaldehyde release assay). It was found that the IC_{50} value was 0.22 μM, which was highly reproducible (Figure 3D; Figure S11 and Table S6). Moreover, WL12 exhibited selectivity over other JmjC domain-containing proteins, such as PHF8/KDM7B, JHDM2A/KDM3A, JMJD2C/KDM4C, and SMCX/KDM5C (Figure S12). We then examined WL12 effects on JMJD6-mediated demethylation in cultured cells. To this end, HeLa

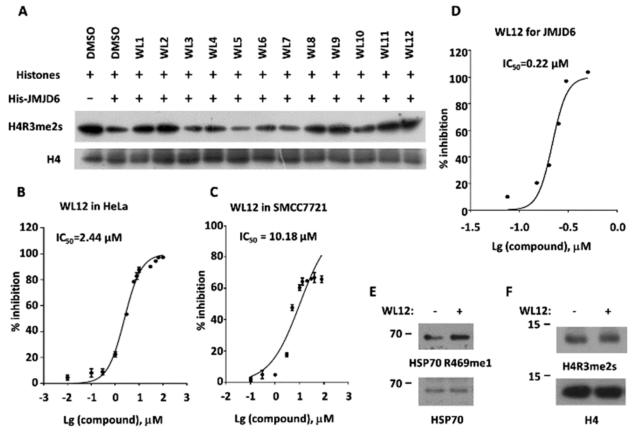

Figure 3. (A) Demethylation assay was performed by mixing purified, bacterially expressed JMJD6 with core histones in the presence or absence of compound WL1 to WL12 (10 μM) followed by immunoblotting with antibodies as indicated. H4R3me2s: histone H4 arginine 3 symmetrical dimethylation. H4: histone H4. (B,C) HeLa (B) and SMCC7721 (C) cells were treated with compound WL12 at concentrations as indicated for 72 h followed by cell proliferation assay. (D) Demethylation assay was performed by mixing purified, bacterially expressed JMJD6 with core histones in the presence or absence of compound WL12 at different concentrations as indicated followed by formaldehyde release measurement. IC_{50} was shown as indicated. The experiment was repeated three times, and representative data was shown. The raw data and the IC_{50} for the other two repeats were shown in Table S6 and Figure S10, respectively. (E,F) HeLa cells were treated with or without WL12 (10 μM) for 6 h followed by immunoblotting assay using antibodies as indicated. Molecular weight was indicated on the left. HSP70, heat shock protein 70; HSP70 R469me1, HSP70 with monomethylated arginine (R)-469.

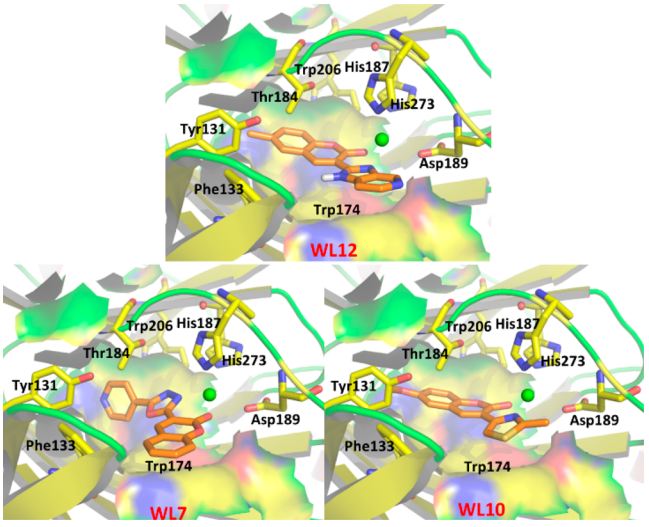

Figure 4. Binding modes of compound WL7, WL10, and WL12 with JMJD6. Residues interacting with ligands were shown by yellow sticks (3ldb).[13] The 2OG-binding site was shown as a yellow surface.

cells were treated with or without WL12 followed by immunoblotting to examine the levels of H4R3me2s as well as HSP70R469me1, which is a nonhistone protein substrate we reported previously.[34] As expected, WL12 treatment led to a significantly increase of HSP70R469me1, which was presumably through inhibiting JMJD6 (Figure 3E). However, no dramatic change of H4R3me2s was observed (Figure 3F),

DOI: 10.1021/acsmedchemlett.9b00264
ACS Med. Chem. Lett. 2019, 10, 1609−1613

which was consistent with our previous report that JMJD6 exhibits no global impact on histone methylation. Instead, it functions only on specific gene loci.[32] Finally, we demonstrated that WL12 was able to bind with JMJD6 examined by Biacore assay (Figure S13). Taken together, our structure-based virtual screening was successful in discovering JMJD6 inhibitors for future structural optimization.

We then examined the binding mode of WL12 with JMJD6 in more details. As shown in Figure 4, the docking pose of WL12 occupied the core 2OG-binding region perfectly. The coumarin and pyrazole rings both formed coordination interactions with iron (Figure S13). The fused benzyl ring in the coumarin group inserted into the inner pocket, forming an $\sigma-\pi$ interaction with Trp206. The pyridopyrazole ring made an $\pi-\pi$ stacking interaction with Trp174. These interaction features well matched the pharmacophore model except that the HB feature projected to Lys204 was missed. Compound WL10 with the same coumarin scaffold as WL12 also made $\pi-\pi$ stacking with Trp174, but the stacking distance for WL10 was longer than WL12 (Figure S14). WL7, another analogue of WL12, exhibited the opposite binding pose to WL12 so that it hardly showed any activity against JMJD6. The binding modes of WL7, WL10, and WL12 were also investigated by MD simulations. The RMSDs indicated that JMJD6 was stable when binding with WL12 (Figure S15A). The RMSDs for the heavy atoms of WL12 were about 0.5 Å relative to the docking pose (Figure S14B). The distance between iron and WL12 was always maintained at a valid window from 2.0 to 2.3 Å for coordination interaction (Figure S16).[35] However, only the coumarin−iron coordination interaction was maintained along the simulation. The Trp174-mediated $\pi-\pi$ stacking was maintained along the simulation according to the distance between the pyridine ring of WL12 and the indole ring of Trp174 (Figure S15C). The simulations suggested that WL7 and WL10 were weaker than WL12 in terms of protein and ligand flexibility (Figures S15A,B). The structure of the catalytic triad was even deformed when the two compounds were bound (Figure S16).

In conclusion, our analysis revealed that the 2OG-binding site of JMJD6 is a druggable pocket for ligand binding. Following our virtual screening protocol, several small-molecule inhibitors capable of inhibiting JMJD6 demethylase activity *in vitro* were discovered. Among them, inhibitor WL12 was shown to be able to suppress JMJD6-dependent cancer cell proliferation including cervical and liver cancer cells, providing a small-molecule probe for studying the biological functions of JMJD6 in cancer development. We envision that a campaign seeking JMJD6 inhibitors to treat cancers will begin following our study.

■ ASSOCIATED CONTENT

Supporting Information

The Supporting Information is available free of charge at https://pubs.acs.org/doi/10.1021/acsmedchemlett.9b00264.

Computational and experimental methods, assay protocols, and supplementary tables and figures (PDF)

■ AUTHOR INFORMATION

Corresponding Author

*Tel: +86-0592-2881146. Fax: +86-0592-2881146. E-mail: w2liu@xmu.edu.cn (W.L).

ORCID

Ting Ran: 0000-0002-1387-4634

Haoliang Yuan: 0000-0003-0248-4347

Wen Liu: 0000-0003-3434-4162

Author Contributions

⊥These authors contributed equally.

Notes

The authors declare no competing financial interest.

■ ACKNOWLEDGMENTS

This work was supported by National Natural Science Foundation of China (81861130370, 81761128015, 31871319, and 21907081), Fujian Province Health Education Joint Research Project (WKJ2016-2-09), Xiamen Science and Technology Project (2017S0091), Xiamen Science and Technology major project (3502Z20171001-20170302), the Fundamental Research Funds for the Central University (20720190145, 2013121036), Fujian Provincial Key Laboratory of Innovative Drug Target Research Funds, "985 project" Funds and "Thousand Young Talents Program" Funds, and Educational Research Projects for Young and Middle-aged Teachers in Fujian Province (JAT170010).

■ REFERENCES

(1) Klose, R. J.; Kallin, E. M.; Zhang, Y. JmjC-domain-containing proteins and histone demethylation. *Nat. Rev. Genet.* **2006**, *7*, 715−727.

(2) Wilkins, S. E.; Islam, M. S.; Gannon, J. M.; Markolovic, S.; Hopkinson, R. J.; Ge, W.; Schofield, C. J.; Chowdhury, R. JMJD5 is a human arginyl C-3 hydroxylase. *Nat. Commun.* **2018**, *9*, 1180−1191.

(3) Webby, C. J.; Wolf, A.; Gromak, N.; Dreger, M.; Kramer, H.; Kessler, B.; Nielsen, M. L.; Schmitz, C.; Butler, D. S.; Yates, J. R., 3rd; Delahunty, C. M.; Hahn, P.; Lengeling, A.; Mann, M.; Proudfoot, N. J.; Schofield, C. J.; Bottger, A. Jmjd6 catalyses lysyl-hydroxylation of U2AF65, a protein associated with RNA splicing. *Science* **2009**, *325*, 90−93.

(4) Walport, L. J.; Hopkinson, R. J.; Chowdhury, R.; Schiller, R.; Ge, W.; Kawamura, A.; Schofield, C. J. Arginine demethylation is catalysed by a subset of JmjC histone lysine demethylases. *Nat. Commun.* **2016**, *7*, 11974−11985.

(5) McAllister, T. E.; England, K. S.; Hopkinson, R. J.; Brennan, P. E.; Kawamura, A.; Schofield, C. J. Recent Progress in Histone Demethylase Inhibitors. *J. Med. Chem.* **2016**, *59*, 1308−1329.

(6) Maes, T.; Carceller, E.; Salas, J.; Ortega, A.; Buesa, C. Advances in the development of histone lysine demethylase inhibitors. *Curr. Opin. Pharmacol.* **2015**, *23*, 52−60.

(7) Chang, B.; Chen, Y.; Zhao, Y.; Bruick, R. K. JMJD6 is a histone arginine demethylase. *Science* **2007**, *318*, 444−447.

(8) Liu, X.; Si, W.; Liu, X.; He, L.; Ren, J.; Yang, Z.; Yang, J.; Li, W.; Liu, S.; Pei, F.; Yang, X.; Sun, L. JMJD6 promotes melanoma carcinogenesis through regulation of the alternative splicing of PAK1, a key MAPK signaling component. *Mol. Cancer* **2017**, *16*, 175−192.

(9) Wang, F.; He, L.; Huangyang, P.; Liang, J.; Si, W.; Yan, R.; Han, X.; Liu, S.; Gui, B.; Li, W.; Miao, D.; Jing, C.; Liu, Z.; Pei, F.; Sun, L.; Shang, Y. JMJD6 promotes colon carcinogenesis through negative regulation of p53 by hydroxylation. *PLoS Biol.* **2014**, *12*, e1001819−e1001836.

(10) Zhang, J.; Ni, S. S.; Zhao, W. L.; Dong, X. C.; Wang, J. L. High expression of JMJD6 predicts unfavorable survival in lung adenocarcinoma. *Tumor Biol.* **2013**, *34*, 2397−2401.

(11) Wan, J.; Liu, H.; Yang, L.; Ma, L.; Liu, J.; Ming, L. JMJD6 promotes hepatocellular carcinoma carcinogenesis by targeting CDK4. *Int. J. Cancer* **2019**, *144*, 2489−2500.

(12) Gao, W. W.; Xiao, R. Q.; Zhang, W. J.; Hu, Y. R.; Peng, B. L.; Li, W. J.; He, Y. H.; Shen, H. F.; Ding, J. C.; Huang, Q. X.; Ye, T. Y.; Li, Y.; Liu, Z. Y.; Ding, R.; Rosenfeld, M. G.; Liu, W. JMJD6 licenses

DOI: 10.1021/acsmedchemlett.9b00264
ACS Med. Chem. Lett. 2019, 10, 1609−1613

ERalpha-eependent enhancer and coding gene activation by modulating the recruitment of the CARM1/MED12 co-activator complex. *Mol. Cell* **2018**, *70*, 340−357.
(13) Hong, X.; Zang, J.; White, J.; Wang, C.; Pan, C. H.; Zhao, R.; Murphy, R. C.; Dai, S.; Henson, P.; Kappler, J. W.; Hagman, J.; Zhang, G. Interaction of JMJD6 with single-stranded RNA. *Proc. Natl. Acad. Sci. U. S. A.* **2010**, *107*, 14568−14572.
(14) Mantri, M.; Krojer, T.; Bagg, E. A.; Webby, C. A.; Butler, D. S.; Kochan, G.; Kavanagh, K. L.; Oppermann, U.; McDonough, M. A.; Schofield, C. J. Crystal structure of the 2-oxoglutarate- and Fe(II)-dependent lysyl hydroxylase JMJD6. *J. Mol. Biol.* **2010**, *401*, 211−222.
(15) Markolovic, S.; Leissing, T. M.; Chowdhury, R.; Wilkins, S. E.; Lu, X.; Schofield, C. J. Structure-function relationships of human JmjC oxygenases-demethylases versus hydroxylases. *Curr. Opin. Struct. Biol.* **2016**, *41*, 62−72.
(16) Hong, X.; Zang, J.; White, J.; Wang, C.; Pan, C. H.; Zhao, R.; Murphy, R. C.; Dai, S.; Henson, P.; Kappler, J. W.; Hagman, J.; Zhang, G. Interaction of JMJD6 with single-stranded RNA. *Proc. Natl. Acad. Sci. U. S. A.* **2010**, *107*, 14568−14572.
(17) Hahn, P.; Böse, J.; Edler, S.; Lengeling, A. Genomic structure and expression of Jmjd6 and evolutionary analysis in the context of related JmjC domain containing proteins. *BMC Genomics* **2008**, *9*, 293−293.
(18) Huang, Y.; Chen, D.; Liu, C.; Shen, W.; Ruan, Y. Evolution and conservation of JmjC domain proteins in the green lineage. *Mol. Genet. Genomics* **2016**, *291*, 33−49.
(19) Halgren, T. A. Identifying and characterizing binding sites and assessing druggability. *J. Chem. Inf. Model.* **2009**, *49*, 377−389.
(20) Ngan, C. H.; Bohnuud, T.; Mottarella, S. E.; Beglov, D.; Villar, E. A.; Hall, D. R.; Kozakov, D.; Vajda, S. FTMAP: extended protein mapping with user-selected probe molecules. *Nucleic Acids Res.* **2012**, *40*, W271−W275.
(21) Lu, S.; He, X.; Ni, D.; Zhang, J. Allosteric modulator discovery: From serendipity to structure-based design. *J. Med. Chem.* **2019**, *62*, 6405−6421.
(22) Lu, S.; Ji, M.; Ni, D.; Zhang, J. Discovery of hidden allosteric sites as novel targets for allosteric drug design. *Drug Discovery Today* **2018**, *23*, 359−365.
(23) Lu, S.; Zhang, J. Small molecule allosteric modulators of G-Protein-Coupled Receptors: Drug-Target interactions. *J. Med. Chem.* **2019**, *62*, 24−45.
(24) Lu, S.; Shen, Q.; Zhang, J. Allosteric methods and their applications: Facilitating the discovery of allosteric drugs and the investigation of allosteric mechanisms. *Acc. Chem. Res.* **2019**, *52*, 492−500.
(25) Friesner, R. A.; Banks, J. L.; Murphy, R. B.; Halgren, T. A.; Klicic, J. J.; Mainz, D. T.; Repasky, M. P.; Knoll, E. H.; Shelley, M.; Perry, J. K.; Shaw, D. E.; Francis, P.; Shenkin, P. S. Glide: a new approach for rapid, accurate docking and scoring. 1. Method and assessment of docking accuracy. *J. Med. Chem.* **2004**, *47*, 1739−1749.
(26) Bavetsias, V.; Lanigan, R. M.; Ruda, G. F.; Atrash, B.; McLaughlin, M. G.; Tumber, A.; Mok, N. Y.; Le Bihan, Y. V.; Dempster, S.; Boxall, K. J.; Jeganathan, F.; Hatch, S. B.; Savitsky, P.; Velupillai, S.; Krojer, T.; England, K. S.; Sejberg, J.; Thai, C.; Donovan, A.; Pal, A.; Scozzafava, G.; Bennett, J. M.; Kawamura, A.; Johansson, C.; Szykowska, A.; Gileadi, C.; Burgess-Brown, N. A.; von Delft, F.; Oppermann, U.; Walters, Z.; Shipley, J.; Raynaud, F. I.; Westaway, S. M.; Prinjha, R. K.; Fedorov, O.; Burke, R.; Schofield, C. J.; Westwood, I. M.; Bountra, C.; Muller, S.; van Montfort, R. L.; Brennan, P. E.; Blagg, J. 8-Substituted pyrido[3,4-d]pyrimidin-4(3H)-one derivatives as potent, cell permeable, KDM4 (JMJD2) and KDM5 (JARID1) histone lysine demethylase inhibitors. *J. Med. Chem.* **2016**, *59*, 1388−1409.
(27) Johansson, C.; Velupillai, S.; Tumber, A.; Szykowska, A.; Hookway, E. S.; Nowak, R. P.; Strain-Damerell, C.; Gileadi, C.; Philpott, M.; Burgess-Brown, N.; Wu, N.; Kopec, J.; Nuzzi, A.; Steuber, H.; Egner, U.; Badock, V.; Munro, S.; LaThangue, N. B.; Westaway, S.; Brown, J.; Athanasou, N.; Prinjha, R.; Brennan, P. E.; Oppermann, U. Structural analysis of human KDM5B guides histone demethylase inhibitor development. *Nat. Chem. Biol.* **2016**, *12*, 539−545.
(28) Hopkinson, R. J.; Tumber, A.; Yapp, C.; Chowdhury, R.; Aik, W.; Che, K. H.; Li, X. S.; Kristensen, J. B. L.; King, O. N. F.; Chan, M. C.; Yeoh, K. K.; Choi, H.; Walport, L. J.; Thinnes, C. C.; Bush, J. T.; Lejeune, C.; Rydzik, A. M.; Rose, N. R.; Bagg, E. A.; McDonough, M. A.; Krojer, T.; Yue, W. W.; Ng, S. S.; Olsen, L.; Brennan, P. E.; Oppermann, U.; Muller-Knapp, S.; Klose, R. J.; Ratcliffe, P. J.; Schofield, C. J.; Kawamura, A. 5-Carboxy-8-hydroxyquinoline is a broad spectrum 2-oxoglutarate oxygenase inhibitor which causes iron translocation. *Chem. Sci.* **2013**, *4*, 3110−3117.
(29) Korczynska, M.; Le, D. D.; Younger, N.; Gregori-Puigjane, E.; Tumber, A.; Krojer, T.; Velupillai, S.; Gileadi, C.; Nowak, R. P.; Iwasa, E.; Pollock, S. B.; Ortiz Torres, I.; Oppermann, U.; Shoichet, B. K.; Fujimori, D. G. Docking and linking of fragments to discover jumonji histone demethylase inhibitors. *J. Med. Chem.* **2016**, *59*, 1580−1598.
(30) Wolber, G.; Langer, T. LigandScout: 3-D pharmacophores derived from protein-bound ligands and their use as virtual screening filters. *J. Chem. Inf. Model.* **2005**, *45*, 160−169.
(31) Pouliot, M.; Jeanmart, S. Pan Assay Interference Compounds (PAINS) and Other Promiscuous Compounds in Antifungal Research. *J. Med. Chem.* **2016**, *59*, 497−503.
(32) Liu, W.; Ma, Q.; Wong, K.; Li, W.; Ohgi, K.; Zhang, J.; Aggarwal, A. K.; Rosenfeld, M. G. Brd4 and JMJD6-associated anti-pause enhancers in regulation of transcriptional pause release. *Cell* **2013**, *155*, 1581−1595.
(33) Zheng, H.; Tie, Y.; Fang, Z.; Wu, X.; Yi, T.; Huang, S.; Liang, X.; Qian, Y.; Wang, X.; Pi, R.; Chen, S.; Peng, Y.; Yang, S.; Zhao, X.; Wei, X. Jumonji domain-containing 6 (JMJD6) identified as a potential therapeutic target in ovarian cancer. *Signal Transduct. Target. Ther.* **2019**, *4*, 24−37.
(34) Gao, W. W.; Xiao, R. Q.; Peng, B. L.; Xu, H. T.; Shen, H. F.; Huang, M. F.; Shi, T. T.; Yi, J.; Zhang, W. J.; Wu, X. N.; Gao, X.; Lin, X. Z.; Dorrestein, P. C.; Rosenfeld, M. G.; Liu, W. Arginine methylation of HSP70 regulates retinoid acid-mediated RARbeta2 gene activation. *Proc. Natl. Acad. Sci. U. S. A.* **2015**, *112*, E3327−E3336.
(35) Rastogi, N.; Singh, A.; Singh, P. K.; Tyagi, T. K.; Pandey, S.; Shin, K.; Kaur, P.; Sharma, S.; Singh, T. P. Structure of iron saturated C-lobe of bovine lactoferrin at pH 6.8 indicates a weakening of iron coordination. *Proteins: Struct., Funct., Genet.* **2016**, *84*, 591−599.

DOI: 10.1021/acsmedchemlett.9b00264
ACS Med. Chem. Lett. 2019, 10, 1609−1613